Monte Carlo Simulation of Chain Molecule Adsorption on a Line Defect

M. R. Wattenbarger,[†,‡] V. A. Bloomfield,[*,†] and D. F. Evans[‡]

Department of Biochemistry, University of Minnesota, St. Paul, Minnesota 55108, and Department of Chemical Engineering and Materials Science, University of Minnesota, Minneapolis, Minnesota 55455

Received June 25, 1991; Revised Manuscript Received September 9, 1991

ABSTRACT: Surface roughness, lattice defects, and surface chemical composition may all affect the adsorption behavior and the adsorbed configurations of polymers. We have performed Monte Carlo computer simulations to study the effect of line defects on otherwise homogeneous flat surfaces on chain molecule adsorption. A chain of 20 monomers adsorbs to a flat surface at monomer–surface interaction energies of about 1 kT, and selective adsorption to a line defect occurs at a ratio of line to surface energy of 6.5. The nonuniform adsorption of polymers on surfaces with heterogeneous interaction energies has implications for the selective adsorption of polymers on patterned surfaces and the interpretation of microscopy images.

Introduction

The adsorption of polymer chains has been studied extensively since it is important to many different problems in colloid stabilization, adhesion, thin films, coatings, biocompatibility, and chromatography. The adsorbed layer thickness, monomer distribution in the adsorbed layer, and fraction of monomers in tails, loops, and trains have been calculated for chains adsorbed on smooth surfaces as functions of chain length and solvent quality.[1-3] Since adsorption on smooth homogeneous surfaces has been fairly well characterized and most real surfaces are rough and heterogeneous, more work is now being done to investigate the effect of surface structure and composition on adsorption. For atoms and small molecules, experimental and theoretical work has shown the role of the surface on processes such as the preferential nucleation of atom clusters on steps,[4] restructuring of surfaces by atom and molecule adsorption,[5] and ordering of molecules in adsorbed layers.[6] These surface phenomena may also be significant in macromolecule adsorption. Theoretical work on polymer adsorption to rough surfaces[7-10] and surfaces with heterogeneous adsorption sites[11] has predicted enhanced adsorption to rough surfaces and segregation of molecules among binding sites.

We are interested in the adsorption of polymers to structured surfaces in order to investigate the possibilities for creating ordered polymer surfaces and to understand adsorption in general. The ability to create ordered arrays of polymers on a substrate would allow the manufacture of polymer films and devices with unique material properties. One major limitation in polymer adsorption studies has been the difficulty in characterizing the surface structure before and after adsorption occurs. Scanning tunneling microscopy (STM) and atomic force microscopy (AFM), which have the potential to image surfaces with nearly atomic resolution, may now be used to characterize the detailed surface structure and may provide valuable information on the adsorption process.[12,13] Pits and lines may also be created with STM and AFM in order to make well-characterized rough surfaces.[14-16] Thus, theoretical work combined with STM and AFM may be able to provide information that will elucidate the mechanism of adsorption on structured surfaces.

A second motivation for this work is to understand the effect of the substrate on molecular imaging in STM and AFM. Most of the STM work on molecular configurations has been done using highly oriented pyrolytic graphite (HOPG) as a substrate since it has large atomically flat areas and the basal plane has very low reactivity. Yet manual cleavage of HOPG is known to create steps and lattice defects which may increase the surface roughness and create ledges with much higher reactivity than the basal plane.[17] The steps and defects interact with adsorbate molecules much more strongly than the flat basal plane and may cause preferential adsorption to the surface defects. The preferential adsorption to defects may significantly alter the configuration on the atomic level from that expected for a molecule on a homogeneous, low-reactivity surface. Thus, the defects may play a large role in the actual configurations of macromolecules observed in STM images made with graphite substrate.

To illuminate these issues, we have modeled the adsorption of a single-chain molecule to a stepped surface with Monte Carlo computer simulations. The step is represented by a line which has a higher interaction energy for the chain monomers than the other surface atoms. The mean square radius of gyration components in the x, y, and z directions were calculated for ranges of surface–monomer and line-defect–monomer interaction energies in order to identify the energies at which preferential adsorption to the line becomes significant.

Computational Methods and Results

Short-chain molecules were represented with a bead–stick type of model in continuous three-dimensional space, as described by Baumgärtner.[18] The excluded volume of the beads was represented by a repulsive potential between monomers on the same chain, defined by

$$U_m = 4\epsilon_m \frac{\sigma_m^{12}}{r^{12}} \qquad (1)$$

The interaction parameters $\epsilon_m = 10$ kT and $\sigma_m = 1.4$ were chosen and no attractive component was included in order to model relatively stiff extended chains such as DNA.

The configurations were generated by first creating ideal chains with no excluded volume constraints. Monomers were added in a randomly chosen direction from the previous monomer until the desired chain length was reached. Then the chains were expanded into a real chain

[†] University of Minnesota, St. Paul.
[‡] University of Minnesota, Minneapolis.

0024-9297/92/2225-0261$03.00/0

Table I
Radius of Gyration for Bulk and Adsorbed Chains

	$\langle RG^2 \rangle$	$\langle RG_x^2 \rangle$	$\langle RG_y^2 \rangle$	$\langle RG_z^2 \rangle$	chains
		a. Bulk Chains			
$N = 20$	18.5 ± 3.86	5.85 ± 4.58	6.69 ± 4.92	5.99 ± 4.55	180
$N = 30$	32.2 ± 9.2	10.5 ± 8.4	11.6 ± 8.7	10.1 ± 8.6	600
$N = 40$	47.2 ± 14.8	15.5 ± 11.8	16.8 ± 14.7	15.0 ± 11.7	360
		b. Adsorbed Chains			
$E_s/kT = 1.01$	20.4 ± 4.54	1.19 ± 2.37	9.93 ± 6.72	9.26 ± 6.68	540
$E_s/kT = 2.30$	22.2 ± 4.49	0.058 ± 0.121	10.8 ± 7.21	11.4 ± 7.55	540
$E_s/kT = 4.60$	22.1 ± 4.7	0.019 ± 0.011	11.2 ± 7.37	10.9 ± 7.32	480
		c. Line Defect ($E_s/kT = 1.01$)			
$E_l/E_s = 6.50$	27.0 ± 4.19	0.342 ± 1.47	1.49 ± 3.50	25.2 ± 7.30	360
$E_l/E_s = 7.24$	28.4 ± 2.81	0.097 ± 0.61	0.825 ± 2.49	27.5 ± 5.18	240
$E_l/E_s = 10.87$	29.0 ± 1.63	0.030 ± 0.16	0.489 ± 1.88	28.5 ± 3.17	240

by moving a randomly chosen monomer, calculating the total monomer repulsion force, and selecting the lowest energy configuration in a Metropolis algorithm. The ideal chains expanded into real chains with excluded volume constraints after approximately 20 000 cycles. The new configurations were generated by moving monomers with a kink-jump method similar to that used by Baumgärtner.[18] The mean square radius of gyration $\langle RG^2 \rangle$ and the components in the x, y, and z directions ($\langle RG_x^2 \rangle$, $\langle RG_y^2 \rangle$, and $\langle RG_z^2 \rangle$, respectively) were calculated with the following equations. x is perpendicular to the surface, and z lies parallel to the line defect.

$$\langle RG_x^2 \rangle = \frac{1}{N}\sum_{i=1}^{N}(x_i - x_{cm})^2 \tag{2}$$

$$\langle RG_y^2 \rangle = \frac{1}{N}\sum_{i=1}^{N}(y_i - y_{cm})^2 \tag{3}$$

$$\langle RG_z^2 \rangle = \frac{1}{N}\sum_{i=1}^{N}(z_i - z_{cm})^2 \tag{4}$$

$$\langle RG^2 \rangle = \langle RG_x^2 \rangle + \langle RG_y^2 \rangle + \langle RG_z^2 \rangle \tag{5}$$

Here x_{cm}, y_{cm}, and z_{cm} are the coordinates of the chain center of mass, and N is the chain length.

Bulk Polymers. Chains were generated for lengths of 20, 30, and 40 monomers. A least-squares analysis of ln $\langle RG^2 \rangle$ vs ln N for bulk chains gives a slope of 1.356, which indicates that the power law exponent is 0.68. The short chain length and chain stiffness make the exponent a little larger than the expected value of 0.6 for a random coil with excluded volume. However, no rigorous conclusions may be drawn concerning the exponent since an exhaustive simulation with a large number of chains was not done. The data for the components of $\langle RG^2 \rangle$ are presented in Table Ia, and a typical chain configuration is shown in Figure 1. The large standard deviations for $\langle RG_x^2 \rangle$, $\langle RG_y^2 \rangle$, and $\langle RG_z^2 \rangle$ occur since a particular configuration may be primarily extended in one direction. The values for $\langle RG_x^2 \rangle$, $\langle RG_y^2 \rangle$, and $\langle RG_z^2 \rangle$ are approximately equal, as must be the case for an ensemble of chains in bulk solution.

Polymers Adsorbed to Flat Surface. The adsorption of chains with 20 monomers to a smooth surface was simulated to determine the surface interaction energy required for adsorption. Chains of 20 rather than 30 or 40 monomers were used since less computational time was required and similar adsorption behavior was expected for all three chain lengths. The chain–surface potential was calculated with a Lennard-Jones potential integrated over the solid surface

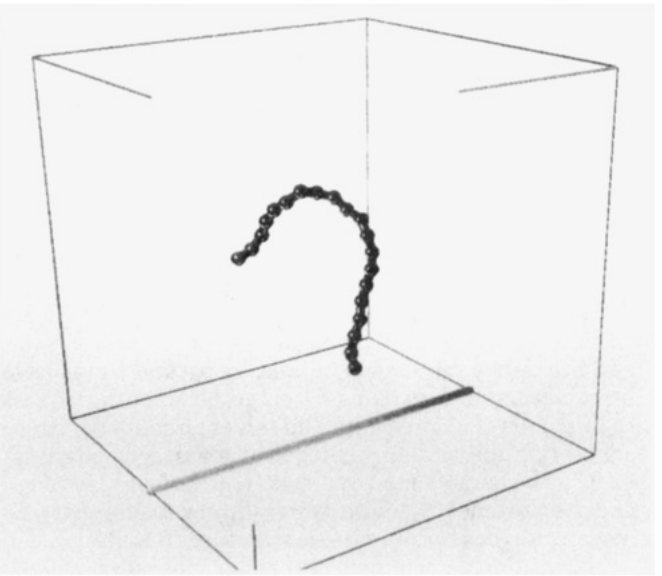

Figure 1. Typical chain configuration for unadsorbed chain with $N = 20$ monomers. The outline of the 3D box and the line defect on the bottom surface are shown.

$$U_{m-s} = \frac{2}{3}\pi\epsilon_s\rho_s\sigma_s^6\left(\frac{2}{15}\frac{\sigma^6}{r^9} - \frac{1}{r^3}\right) \tag{6}$$

where σ_s and ϵ_s are the chain–surface interaction parameters and ρ_s is the density of atoms in the solid.[19] All lengths are measured in units of the bond length. A density of 0.38 atoms/(bond length)^3 was used in order to model a graphite lattice (open face hexagonal packed lattice). Note that the maximum well depth corresponds to $2.3\epsilon_s$ instead of ϵ_s. The quantity $E_s = 2.3\epsilon_s$ will be used to represent the maximum surface interaction energy.

The chains are placed in a cubic box of length L, and the surface is located in the y–z plane at $x = 0.0$. The box sides have periodic boundary conditions for the $y = 0, L$ and $z = 0, L$ planes perpendicular to the adsorbing surface. The top of the box at $x = L$ has a reflecting boundary to keep all the chains within the box. The box length is calculated as a function of the number of monomers so that a chain may not interact with a periodic image of itself in another box

$$L > N + R_c \tag{7}$$

where R_c is the cutoff distance for the monomer–monomer potential ($R_c = 2.5$).

The chain configurations which were generated for the bulk chain molecules were used as the initial configurations in the adsorption simulations. Each chain was placed with the monomer closest to the surface at a distance within

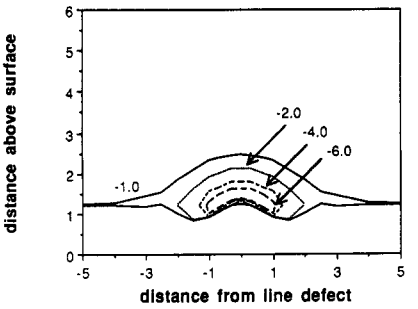

Figure 2. Curves of constant potential energy above a line defect for $E_s/kT = 1.0$ and $E_l/kT = 7.24$. The minimum energy of −1.0 kT above the flat surface and the symmetric closed curves of lower minimum energy near the line defect are shown. The potential decays to zero at distances greater than those shown by the upper −1.0 curve and increases to large positive values at distances less than those indicated by the lower −1.0 curve.

the interaction potential of the surface at the beginning of the adsorption run. The monomers were randomly chosen and moved according to a Monte Carlo algorithm, and the average parameters of radius of gyration, position of the center of mass, bond correlation, and average energy were monitored. Interactions between different chains were not considered since only single-chain adsorption was modeled. Once a steady state for all of the variables was reached, the system was defined to be in an equilibrium state. Subsequent sets of chain configurations generated by Monte Carlo simulation were separated from the previous set by an interval of 80 000 cycles since at that interval the average bond correlation with the previous set of chains had reached a minimum value. The average parameters reported for each surface energy were obtained by averaging a total of 480–540 different configurations. The results are summarized in Table Ib.

Polymers Adsorbed to Surface with a Line Defect. Adsorption to the surface line defect was modeled by adding a high-energy line at $x = 0.0$ and $y = 0.5L$ on the adsorbing surface of the box. The Lennard-Jones potential integrated over the line is

$$U_{m-l} = 4\epsilon_l\rho_l\sigma_l^6\left(\frac{1}{11}\frac{\sigma_l^6}{r^{11}} - \frac{1}{5}\frac{1}{r^5}\right) \quad (8)$$

where σ_l and ϵ_l are the line-defect interaction parameters. Note that, for this potential, the maximum surface energy per monomer E_l is $0.611\epsilon_l$.

Each chain was positioned so that the monomer closest to the wall was at $y = 0.5$ and within the distance for the surface interaction potential at the beginning of the adsorption. New chain configurations were generated for (1–2) × 10^6 cycles until the average properties clearly diverged or converged. The results for the radius of gyration are summarized in Table Ic for line energies at which the an equilibrium state was reached. The radius of gyration was calculated for two sets of chain configurations separated by 180 000, 240 000, or 360 000 cycles in each simulation. Each simulation was repeated for a different set of initial configurations to confirm that the equilibrium values were independent of the initial conditions. Similar equilibrium values were found in each of the repeated simulations.

The curves of constant potential energy ($U_{m-s} + U_{m-l}$) above an adsorbing surface with a line defect are shown in Figure 2 for $E_s/kT = 1.01$ and $E_l/kT = 7.24$. The surface is located perpendicular to the plane of the plot on the horizontal axis at 0 units above the surface, and the projection of the line defect onto the figure is at the (0,0) point. On the homogeneous surface, the minimum energy

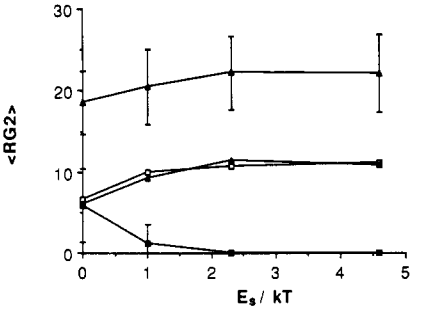

Figure 3. Radius of gyration and components in x, y, and z directions of chains adsorbed to surfaces with energies E_s/kT: (△) $\langle RG^2\rangle$, (▲) $\langle RG_z^2\rangle$, (□) $\langle RG_y^2\rangle$, and (■) $\langle RG_x^2\rangle$. Error bars are shown for $\langle RG^2\rangle$ and $\langle RG_x^2\rangle$. x is perpendicular to the surface, and z lies parallel to the line defect. $N = 20$ monomers.

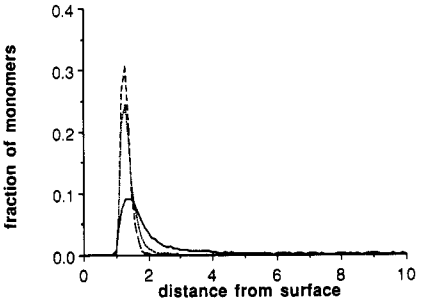

Figure 4. Monomer distribution above the surface for chains on surfaces with E_s/kT = (—) 1.0, (···) 2.3, and (- -) 4.6.

occurs at 1.2 units above the surface. Near the line defect, there is a region with symmetric closed curves of lower minimum energies. The −1.0 curve bifurcates above the line defect since the energy is lower there than on the flat surface. At distances above the surface greater than those indicated by the upper −1.0 curve, the potential decays to zero. The minimum in the potential (8.24 kT) is reached at a distance of 1.2 bond units above the surface and ±0.72 bond units on the horizontal axis from the line. At distances closer to the surface below the lower −1.0 curve, the potential increases and becomes repulsive. The potential energy minimum corresponds to an energy of $E_l + E_s$; however, the data will be analyzed by the ratio E_l/E_s.

Analysis of Results

The effect of the surface interaction energy on adsorption to a smooth surface may be seen in the change in the radius of gyration with energy shown in Figure 3. At $E_l = 0.0$, the chains are isotropic in the x, y, and z directions since $\langle RG_x^2\rangle$, $\langle RG_y^2\rangle$, and $\langle RG_z^2\rangle$ are equal when there is no surface energy. $\langle RG_x^2\rangle$ decreases as the surface energy increases, which indicates that the chains are flattening out on the surface. $\langle RG_y^2\rangle$ and $\langle RG_z^2\rangle$ increase slightly since the excluded volume restrictions prevent the overlap of monomers. $\langle RG_x^2\rangle$ approaches a minimum at a surface energy of 2.3 kT and greater, and the standard deviation is very small, which indicates that the chains are nearly two-dimensional. The plots of the monomer distribution above the adsorbing surface in Figure 4 also show the increasing monomer density near the surface as the surface interaction parameter increases. Nearly all of the monomers are in a narrow region near the surface at an energy of 2.3 kT and above.

The adsorption-transition energy is the minimum energy at which the chains remain attached to the surface. The adsorption-transition energy occurs near $E_s/kT = 1.0$ for $N = 20$ since approximately 93% of the chains in the ensemble are adsorbed. Some of the chains in the ensemble

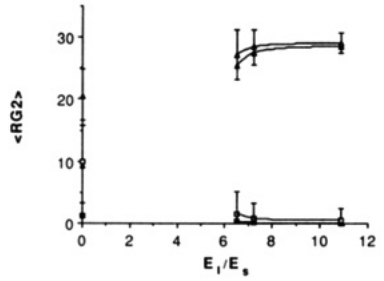

Figure 5. Radius of gyration and components in x, y, and z directions of chains adsorbed to a surface with $E_s/kT = 1.0$ and various ratios of E_l/E_s: (△) $\langle RG^2 \rangle$, (▲) $\langle RG_z^2 \rangle$, (□) $\langle RG_y^2 \rangle$, and (■) $\langle RG_x^2 \rangle$. Error bars are shown for $\langle RG^2 \rangle$ and $\langle RG_y^2 \rangle$. N = 20 monomers.

of 180 different configurations did attach and detach from the surface while the average chain parameters were fairly constant. The adsorption-transition energy could not be identified more precisely with this method since a very long equilibration time for many different chains would be required to determine if those which repeatedly attached to and detached from the surface would eventually remain attached to the surface. Yet the model does indicate that at least almost all of the chains preferentially adsorb to the surface when $E_s/kT = 1.01$, a value consistent with other values reported in the literature for chains of 20 monomers.[10,20] For larger N, the adsorption-transition energy is expected to decrease since more monomers are available to interact with the surface. The limiting adsorption-transition energy for infinitely long chains is 0.44 kT.[21]

The surface energy was chosen to have a value near the adsorption-transition energy ($E_s/kT = 1.01$), and the ratio E_l/E_s was varied between 3.62 and 10.87 to determine when chains would preferentially adsorb to the line defect. A plot of the mean square radius of gyration for the line-defect energies which reached an equilibrium state on a surface with $E_s/kT = 1.01$ is shown in Figure 5. For $3.67 \leq E_l/E_s \leq 6$, the chains detached from the line and eventually from the surface as the simulation progressed. The chain dimensions varied as chains diffused into the bulk region and the parameters did not converge, so it was not possible to calculate equilibrium values. For $E_l/E_s = 6.5$, the radius of gyration, energy, and average center of mass distance above the surface reached steady-state values in three different simulations. Almost all of the chains were attached to the line and did not diffuse away from the line. The chains were strongly adsorbed to the line for $E_l/E_s = 10.87$ since very little change in the configurations occurred after the equilibrium state was reached. In the region $6.5 \leq E_l/E_s \leq 10.87$, $\langle RG_z^2 \rangle$ approaches $\langle RG^2 \rangle$ and $\langle RG^2 \rangle$ increases since the chains are becoming rodlike when the chains preferentially adsorb to the line. Likewise, $\langle RG_y^2 \rangle$ and $\langle RG_x^2 \rangle$ decrease as E_l/E_s increases.

A sigmoidal curve is generally expected for plots of chain dimension vs attractive energy (such as in Figures 3 and 5) with a sharp change in the $\langle RG^2 \rangle$ parameters at the adsorption-transition energy. However, since the chains in these simulations were not permanently tethered to the wall, many cycles and different initial chain configurations would be required to gather more extensive, statistically accurate data in the adsorption-transition region. Yet we can estimate a minimum ratio of E_l/E_s for the chains to preferentially adsorb to the line in the initial stages of adsorption which may be a little larger than the actual transition energy.

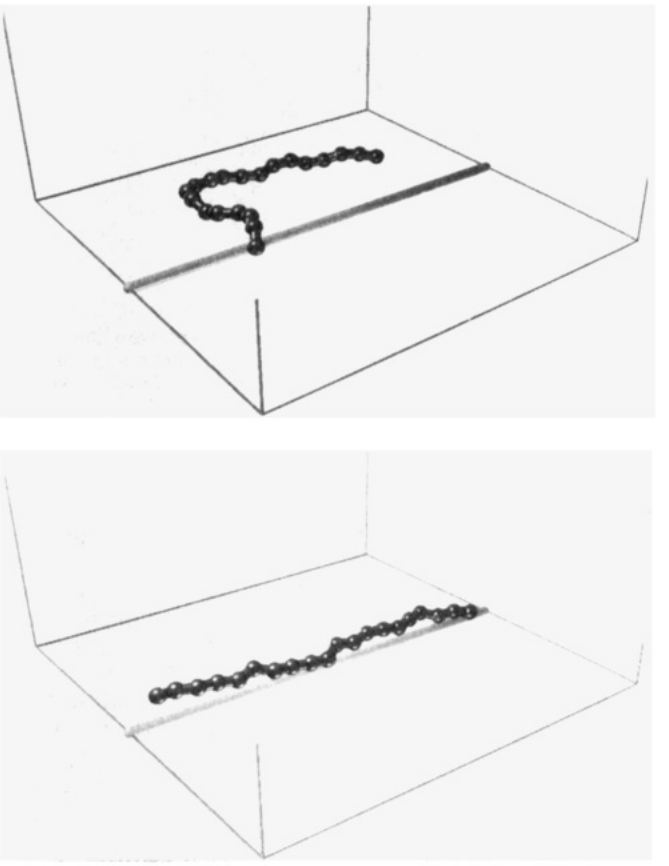

Figure 6. Typical adsorbed chain configurations: (a, top) smooth surface with no line defect, $E_s/kT = 1.0$, (b, bottom) line-defect energy, $E_s/kT = 1.0$ and $E_l/kT = 7.24$. Both chains are lying on the surface. The average distances between the center of the beads and the surface are (a) 2.05 and (b) 1.96 bond units. N = 20 monomers.

Typical configurations for chains adsorbed to a smooth surface and a surface with a line defect are shown in Figure 6. The first configuration (Figure 6a) is for a chain adsorbed to a smooth surface. The chain does not lie in any particular direction with respect to the y or z axis. Figure 6b shows a chain adsorbed to a line with $E_l/E_s = 7.24$. The chain alignment along the line defect is clearly seen.

Conclusions

The results indicate that a chain of 20 monomers may preferentially adsorb along a line rather than on a uniformly flat area when the line energy is at least 6.5 times greater than the surface energy. Experimental measurements of polymer adsorption to surfaces have shown that adding one functional end group to a polymer can cause a nonadsorbing polymer to adsorb. The polymer end group to surface interaction energy was estimated to be 6.4 kT.[22] Thus it may be possible to prepare modified surfaces and polymers in order to cause adsorption in particular surface patterns. Nanolithography techniques along with STM and AFM imaging may be used to investigate these adsorption problems. We are currently pursuing various experimental techniques for creating and characterizing line defects on surfaces for adsorption studies.

There are interesting implications for the interpretation of images from STM and AFM also. While it is not yet possible to measure accurately the interaction potential between a monomer and a surface, it is likely that the actual difference in potential between an edge and the basal plane may be at least a factor of 10. A comparison

of the surface functional groups, double-layer capacity, adsorption, wettability, and electrocatalytic properties between the graphite basal plane and edges have shown that the edges have much higher activity than the basal plane.[23] Also, it is not yet possible to determine if small molecules such as organics are already adsorbed to edges and defects before the sample is placed on the graphite, nor to determine the actual distribution and reactivity of active sites. Yet preferential adsorption of small molecules which have an affinity for macromolecules or adsorption of macromolecules directly to line defects, such as steps or dislocations, may occur. Therefore, the microscopist should be aware of the effect of substrate heterogeneity on molecule adsorption and the consequent possibility of imaging artifacts.

Acknowledgment. We would like to thank the Minnesota Supercomputer Institute for providing computer time and graphics support for this project and the NSF and NIH for funding this work. We would also like to acknowledge the guidance of Dr. Young-Hwa Kim in the initial stage of the project.

References and Notes

(1) Dickinson, E.; Lal, M. *Adv. Mol. Relax. Interact. Processes* **1980**, *1*, 87.
(2) Takahashi, A.; Kawaguchi, M. *Adv. Polym. Sci.* **1982**, *46*, 1.
(3) Ploehn, H. J.; Russel, W. B. *Adv. Chem. Eng.* **1990**, *15*, 137.
(4) Albano, E. V.; Martin, H. O. *Phys. Rev. B* **1987**, *35*, 7820.
(5) Somorjai, G. A.; van Hove, M. A. *Prog. Surf. Sci.* **1989**, *30*, 201.
(6) Binder, K.; Landau, D. P. *Adv. Chem. Phys.* **1989**, *76*, 91.
(7) Edwards, S. F.; Chen, Y. *J. Phys. A: Math. Gen.* **1988**, *21*, 2963.
(8) Douglas, J. F. *Macromolecules* **1989**, *22*, 3707.
(9) Balazs, A. C.; Huang, K.; Lantman, C. W. *Macromolecules* **1990**, *23*, 4641.
(10) Baumgärtner, A.; Muthukumar, M. *J. Chem. Phys.* **1991**, *94*, 4062.
(11) (a) Balazs, A. C.; Huang, K.; McElwain, P.; Brady, J. E. *Macromolecules* **1991**, *24*, 714. (b) Huang, K.; Balazs, A. C. *Phys. Rev. Lett.* **1991**, *66*, 620.
(12) Hansma, P. K.; Elings, V. B.; Marti, O.; Bracker, C. E. *Science* **1988**, *242*, 109.
(13) Gratz, A. J.; Manne, S.; Hansma, P. K. *Science* **1991**, *251*, 1343.
(14) Garfunkel, E.; Rudd, G.; Novak, D.; Wang, S.; Ebert, G.; Greenblatt, M.; Gustafsson, T.; Garofalini, S. H. *Science* **1989**, *246*, 99.
(15) Chang, H.; Bard, A. J. *J. Am. Chem. Soc.* **1990**, *112*, 4598.
(16) Utsugi, Y. *Nature* **1990**, *347*, 747.
(17) Clemmer, C. R.; Beebe, T. P., Jr. *Science* **1991**, *251*, 640.
(18) Baumgärtner, A. *J. Chem. Phys.* **1980**, *72*, 871.
(19) Steele, W. A. *Surf. Sci.* **1973**, *36*, 317.
(20) Birshtein, T. M. *Macromolecules* **1979**, *12*, 715.
(21) Eisenriegler, E.; Kremer, K.; Binder, K. *J. Chem. Phys.* **1982**, *12*, 6296.
(22) Frantz, P.; Leonhardt, C. C.; Granick, S. *Macromolecules* **1991**, *24*, 1868.
(23) Randin, J. In *Encyclopedia of Electrochemistry of the Elements*; Bard, A. J., Ed.; Dekker: New York, 1976; Vol. 7, pp 1–291.